NASA CR-120996

DEVELOPMENT OF A CORE SHEATH PROCESS FOR PRODUCTION OF OXIDE FIBERS

by

Stanley Freske

WHITTAKER CORPORATION

prepared for

NATIONAL AERONAUTICS AND SPACE ADMINISTRATION

NASA Lewis Research Center
Contract NAS 3-14324
Leonard Westfall, Project Manager

FINAL REPORT

DEVELOPMENT OF A CORE SHEATH PROCESS FOR PRODUCTION OF OXIDE FIBERS

by

Stanley Freske

WHITTAKER CORPORATION
Research and Development Division
San Diego, California 92123

prepared for

NATIONAL AERONAUTICS AND SPACE ADMINISTRATION

12 July 1972

Contract NAS 3-14324

NASA Lewis Research Center
Cleveland, Ohio
Leonard Westfall, Project Manager

FOREWORD

The work described herein was done at the Research and Development Division, Whittaker Corporation, under NASA Contract NAS 3-14324 with Mr. Leonard J. Westfall, NASA-Lewis Research Center, as Project Manager. Mr. Stanley Freske was the Whittaker Program Manager and principal investigator.

TABLE OF CONTENTS

ABSTRACT

Improvements were sought in an oxide fiber of a core-sheath configuration, intended for structural applications at 2000°F (1093°C). Discontinuities in the core were eliminated by using core materials other than pure alumina, and thus continuous core-sheath fibers were produced. In the case of some core materials, the continuous sections were sufficiently long for applications in short fiber composites. Creep at 2000°F (1093°C) was found to be due, in most cases, not to creep in the core, but to breaks in the core allowing the glass sheath to creep. The problem of low core strength was not solved; however, evidence was obtained indicating that a closer match between the thermal expansion coefficient of the sheath and the core would greatly improve the strength.

I. SUMMARY

The objective of this work was the development of a core-sheath process for producing an oxide fiber possessing superior mechanical and chemical properties at 2000°F (1093°C) and above. Of the two major difficulties which existed at the outset of the program, mullite sections in the core, and insufficient mechanical performance by the fiber especially at 2000°F (1093°C), only the first was successfully solved.

Several approaches were used in attempts to eliminate the core discontinuities. Increasing the alumina content of the sheath glass was tried, but was found to be too detrimental to the forming process. Lengthening the core orifice nozzle to minimize diffusion of SiO_2 into Al_2O_3 was successful in this respect but sufficiently changed the inherent process so as to cause steeper temperature gradients in the dual bushing assembly. As a result, overheating and melting of several iridium bushings developed before proper control of the temperature was established. Once these problems were overcome, the nozzle lengthening produced a significant improvement in the core. However, the approach which provided the real solution to the problem of core discontinuities consisted of replacing the pure alumina with other, appropriate core compositions. It became obvious later in the contract that the discontinuities were caused by the large volume shrinkage exhibited by alumina during solidification and by thermal expansion mismatches between the core and sheath materials. X-ray data indicated that mullite formation, previously thought to be the primary cause of the discontinuities, did not occur even when the core initially contained silica. Of the new core compositions used in this work, the best appears to have been spinel ($MgO \cdot Al_2O_3$).

Some questions concerning the mechanical performance of the core-sheath fiber were answered, but the basic problem was not solved. The creep observed at 2000°F (1093°C) was a reflection of creep in the core in only a few cases. In most cases, breaks developed in the core, and the creep actually occurred in the glass sheath. Thus, the basic problem is one of low tensile strength of the core. It is considered highly probable that the low strength is in large measure due to the fact that the thermal expansion coefficient of the sheath is almost an order of magnitude smaller than that of the core. Work on increasing the thermal expansion of the sheath glass without decreasing the viscosity was initiated but was not completed.

II. INTRODUCTION

This project constituted a continuation of contract NAS 3-12434* which was a study of the feasibility of manufacturing oxide fibers of a core-sheath configuration for high-temperature structural applications. Although feasibility was proved by the production of samples, two serious problems crystallized out of the preceding project:

1. The composition varied in the core resulting in alternating sections of mullite and sections of relatively pure Al_2O_3 contained in a glass sheath. The alternating two-phase core caused stress concentrations between the phases which resulted in the second problem.

2. Insufficient strength and creep resistance of the fiber in tension, in particular at 2000°F (1093°C).

At the outset of the project reported here, it was felt that the first problem had to be solved before there could be any hope of solving the second, and the work proceeded accordingly. The first problem was believed to be caused by mixing of the liquid core and sheath materials from nozzle flow turbulence and by diffusion. The mixing was minimized by improving the flow and shortening the time at temperature for diffusion during the fiber forming process.

*"Investigation to Develop a Core Sheath Process for Production of Oxide Fibers," NASA CR-72758, 5 August 1970

III. EQUIPMENT AND PROCESS DEVELOPMENT

Changes were made in the basic fiber forming equipment utilized in the performance of the preceding contract, and centered on the bushing (see Fig. 4 of NASA CR-72758). Experimentation centered on materials of manufacture and orifice configuration, and represented about half of the contract effort.

The materials used for the bushing were iridium, tungsten, and molybdenum. Of the three, iridium was the best since it did not react with any of the molten oxides, however its low melting point 4442°F (2450°C) and its very high cost made it less desirable for the outer bushing. Tungsten and molybdenum are lower in cost and have sufficiently high melting temperatures, although both react with the liquid glass. The tungsten bushing was the better of the two.

The diameter of the opening of the outer orifice was decreased to compensate for the lower viscosities produced by composition changes in the glass. It was found that a sheath orifice opening of 0.25 inch (0.62 cm) was adequate for the modified glasses, 5A glass (SiO_2-5% Al_2O_3).

In the search for a method to eliminate the discrete sections of mullite in the fiber core, it was decided to lengthen the core orifice nozzle for the following reasons:

1. The long nozzle injects Al_2O_3 into the molten glass at a point near the bottom of the forming cone. The time of contact between the alumina and the sheath glass with both in the molten state is shortened, thus allowing less time for silica to diffuse into the core.

2. The alumina is injected into the forming cone at a point where the temperature of the glass is lower and the viscosity higher, thus reducing the rate of diffusion of silica into the core. The alumina would remain molten until ejected from the nozzle since it carries a considerable amount of heat with it.

Preliminary experiments using a tungsten rod simulating the nozzle were carried out to determine the extent to which the nozzle could be lengthened without adverse effects on the fiber forming. The temperature gradient along the rod was also determined. A temperature drop of 360°F (200°C) was observed over the first inch below the sheath orifice at normal forming temperature as well as at considerably lower temperatures.

When the new core bushing arrived from the manufacturer, it was found to have a nozzle considerably longer than expected. It projected 1.4 inch (3.56 cm) beyond the sheath orifice as compared to 0.15 - 0.2 inch (0.38 - 0.51 cm) in the case of the original nozzle. When this bushing was tried, the glass flowed along the nozzle and formed a small cone at the tip, just as desired. On the other hand, the alumina could

not be made to flow through the nozzle even though a temperature reading of 3830°F (2110°C) was obtained at the tip of the nozzle, and pressure pulses were superimposed on approximately 12 inches (30.48 cm) of static pressure above the core melt. The nozzle was cut to 1.1 inch (2.79 cm), giving a projection beyond the sheath orifice of 0.8 inch (2.0 cm). In subsequent experiments, two iridium sheath bushings were destroyed through localized melting. Yet, the alumina would not flow, except for an uncontrolled flow which occurred at approximately the time when the first bushing melted. Since the highest temperature reading at the nozzle tip was 3685°F (2030°C) in one case and 3694°F (2035°C) in the other, as compared to the much higher value of 3830°F (2110°C) in the earlier experiment where no such melting occurred, it was conjectured that the localized melting was caused by the development of hot spots on the heating element. Supporting evidence was obtained by sending a current through the element large enough to produce the first red glow, with the furnace chamber open. The glow occurred in a pattern which corresponded quite well to the melting pattern on the first bushing, while the rest of the element remained dark. A different element was used with the second bushing, and was not tested.

The iridium sheath bushing was replaced with a tungsten bushing to avoid further melting. In a subsequent experiment, however, during which a maximum temperature reading of 3750°F (2065°C) was obtained at the nozzle tip, while no flow of alumina was obtained, the core bushing melted. This cannot be explained in terms of hot spots on the heating element. On the other hand, examination of the data shows that the power settings at the time of this occurrence should have produced a temperature considerably higher than that recorded. Factors such as smoke in the furnace chamber or deposit on the sight window, which may go unnoticed, can drastically lower the temperature readings. Whatever the cause of the melting, the indication was clear that a further shortening of the core orifice nozzle was necessary to bring about the flow of alumina.

A complete, new iridium bushing assembly was obtained. The length of the core orifice nozzle was 0.9 inch (2.28 cm) and projected 0.6 inch (1.52 cm) beyond the glass orifice, which had a diameter of 0.25 inch (0.635 cm). The sheath bushing was equipped with four iridium/iridium 50% rhodium thermocouples in an attempt to protect it from excessive temperatures and consequent melting. Furthermore, a heating coil was fashioned from 0.04 inch (0.01 cm) diameter Zirtung* welding electrodes and was placed around the nozzle to reduce the temperature gradient between the bushing and the nozzle tip. Also for the purpose of reducing the temperature gradient, the Zircoa-Cast** bushing support was provided with three large openings to permit radiation from the main heating element to reach the nozzle. The thermocouple readings were consistently more than 360°F (200°C) below the corresponding optical pyrometer readings, and can be assumed to be in error. During the third run, all four thermocouples failed at a temperature of approximately 3632°F (2000°C). The nozzle

* Sylvania Electric Products, Inc.

** Zirconium Corporation of America

heating element had the desired effect of reducing the temperature gradient but, again during the third run, it failed due to oxidation before any attempt at core-sheath fiber forming had been made. In spite of these failures, however, flow of alumina was obtained through this 0.9 inch (2.28 cm) long nozzle. Unfortunately, after several successful runs, localized melting of the sheath bushing did again occur, apparently because during the last run, the temperature was allowed to rise to a value somewhat higher than needed.

Resorting again to a tungsten sheath bushing predictably brought about the darkening of the alumina-containing sheath glass, so objectionable because it interferes with the needed view of the core material as it issues from the nozzle into the glass forming cone. For this reason, a molybdenum bushing was obtained in the hope that the darkening would not occur with the glass in contact with this material instead of tungsten. On the contrary, the darkening was considerably more severe in the case of molybdenum. This bushing also produced an excessive amount of smoke in the furnace chamber and a deposit on the sight window which made meaningful temperature readings during forming difficult or impossible. Furthermore, a reaction definitely took place at the points where the iridium and the molybdenum were in contact. Examination of the bushing after all glass had been removed with hydrofluoric acid showed that some material had disappeared from the support legs of the iridium core bushing and that holes had actually developed in the bottom of the molybdenum bushing at the locations where these legs rested. In addition, the nozzle, including the orifice, was covered with a metallic material, probably molybdenum which could have been deposited through an oxidation-reduction process, or an iridium-molybdenum alloy.

IV. FIBER MANUFACTURE

A. Sheath Compositions

Several problems were encountered which had possible solutions centered on a change in the glass composition. The first problem was that of SiO_2 diffusion into the Al_2O_3 core while both materials were in the liquid state. This problem was attacked by adding Al_2O_3 to the SiO_2 glass to reduce the concentration gradient across the Al_2O_3-SiO_2 boundary. The second problem was the thermal expansion difference between the sheath and the core material. To solve this problem a number of materials were added to the SiO_2 base glass in an attempt to raise its coefficient of thermal expansion while retaining a workable viscosity in the temperature range of 3632°F (2000°C).

An attempt was made to increase the alumina content of the sheath glass for the purpose of reducing the diffusion of silica from the sheath into the alumina core. As mentioned earlier, compensation for the unavoidable decrease in viscosity was provided by reducing the sheath orifice diameter to 0.2 inch (0.51 cm). An alumina content of 10 w/o was used initially, but due to the low viscosity at the temperature required to melt the core alumina, the surface tension of the glass was sufficiently high to pinch off the fiber just below the forming cone. This condition could not, of course, be improved by a reduction in the size of the glass orifice, effective only in helping to control the flow of glass out of the bushing. The alumina content was decreased to 7 w/o and core-sheath fibers were drawn, but at a reduced forming temperature, with readings at the nozzle tip as low as 1950°C. These were inferior fibers with small core-to-sheath ratios and a high frequency of core discontinuities. Finally, the alumina content was reduced to the original level of 5 w/o while the 0.2 inch (0.51 cm) orifice was retained. These fibers were also of inferior quality, prompting the decision to return to an orifice diameter of 0.3 inch (0.76 cm).

At the higher bushing temperatures required after the longer core orifice nozzle had been introduced, the viscosity even of the 5A-glass was too low. Thus, a glass containing only 3 w/o alumina (3A-glass) was tried, and was found to have ideal forming characteristics. This glass was found to have the added advantage of exhibiting considerably less darkening than the 5A-glass when contained in tungsten.

Since early tensile strength measurements had indicated that Vycor* glass was considerably stronger than either 3A- or 5A-glass, Vycor was reintroduced in an attempt to improve fiber properties. The Vycor glass has one distinct advantage in that it remains transparent and colorless in either a tungsten or a molybdenum bushing. The Vycor glass did not wet the core orifice nozzle as easily as the 3A-glass, and it became necessary to use a tungsten probe to effect complete wetting. Core-sheath fibers

* Corning Glass Works

were formed using Vycor in the sheath and spinel, mullite, and alumina in the core, but they generally appeared to be more brittle and contained more cracks and discontinuitites than fibers using 3A-glass. These differences can be accounted for by the Vycor glass having a smaller coefficient of thermal expansion than the 3A-glass.

Since many of the undesirable characteristics of the present core-sheath fiber may be caused by the large difference in thermal expansion between the sheath and the core, an investigation of sheath glass compositions was initiated in an effort to increase the expansion coefficient significantly, but without decreasing the viscosity, not an altogether simple task. For instance, additions of large cations such as the alkaline metals greatly increase thermal expansion, but also drastically reduce viscosity.[1] Several 5-gram batches were mixed and melted in an oxy-hydrogen torch. The first column in Table I gives the amount of additive to silica, expressed in percent by weight. It was decided that at least 10 w/o would be required to increase the viscosity to any significant extent, and this was used as a standard addition. For the purpose of comparing viscosity, each sample was mounted in the torch, and the temperature monitored by means of an optical pyrometer. The temperature readings given in Table I are uncorrected and, of course, significantly below the true temperature values. Since the emissivity of the various glasses may have varied considerably, a platinum bead was deposited on the hot melt in each case, and the temperature readings on these beads were used when comparing viscosity. Estimates of the viscosity were obtained by probing with a tungsten rod; the statements under "Remarks" should be easily interpreted if it is noted that the word "fluid" is used whenever the viscosity was too low to draw fibers, and the word "stiff" whenever it was too high. 5A-glass (first in the table) was used as a reference, since experience has shown that the viscosity of this glass is about as low as can be tolerated.

Five compositions were made but are not included in Table I because studying the viscosity of these would have constituted a wasted effort. One containing 10 w/o TiO_2 and another containing 10 w/o Cr_2O_3 both turned very dark upon melting. This is unacceptable in a sheath glass as explained earlier. One contained 10 w/o WO_3, which apparently did not dissolve in the silica but formed small, dark-blue inclusions in the otherwise clear glass. Finally, both 10 and 20 w/o MoO_3 were used as additions, but in each case density determinations by means of Archimedes' principle showed that virtually all of the MoO_3 volatilized during melting.

As Table I shows, in the case of four compositions, bubbles were generated in the melt. This sometimes occurs when the torch is not adjusted to give a neutral flame, but when proper adjustment does not eliminate the bubbles, volatilization of the additive is indicated. This, too, is unacceptable, and these additives (CaO, BaO, SnO_2, and ZnO) could be eliminated. Of the remaining compositions with a single additive, only the one with MgO appeared to be more fluid than the 5A-glass. This left four: La_2O_3, Ta_2O_3, Y_2O_3, and ZrO_2, each of which appeared more viscous than the 5A-glass. The composition containing Ta_2O_3 unfortunately showed some

TABLE I

PROPERTIES OF SHEATH GLASS COMPOSITIONS

Additive, w/o	Temperature		Remarks
	Glass	Pt Bead	
$5Al_2O_3$	3200°F (1760°C)	3191°F (1755°C)	Slightly too fluid to draw fibers.
10MgO	3182°F (1750°C)	3200°F (1760°C)	Quite fluid.
10CaO	3164°F (1740°C)	3191°F (1755°C)	Quite fluid. Large bubbles.
10BaO	3055°F (1680°C)	3174°F (1745°C)	Quite fluid. Bubbles.
$10La_2O_3$	3128°F (1720°C)	3200°F (1760°C)	Quite stiff.
"	3180°F (1750°C)	3209°F (1765°C)	Fairly stiff.
$10SnO_2$	*	3200°F (1760°C)	Quite stiff. Many bubbles.
$10Ta_2O_5$	3200°F (1760°C)	3200°F (1760°C)	Quite stiff. Striated.
$10Y_2O_3$	3245°F (1785°C)	3191°F (1755°C)	Quite stiff.
10ZnO	*	3191°F (1755°C)	Fairly stiff. Many bubbles.
$10ZrO_2$	3191°F (1755°C)	3191°F (1755°C)	Very stiff.
"	3326°F (1830°C)	3326°F (1830°C)	Quite stiff.
10MgO, $10ZrO_2$	3218°F (1770°C)	3011°F (1655°C)	Very fluid.
$10Al_2O_3$, $10ZrO_2$	3146°F (1730°C)	3038°F (1670°C)	Quite fluid.
$5Al_2O_3$, $10ZrO_2$	3389°F (1865°C)	3191°F (1755°C)	Slightly too fluid to draw fibers.
"	3218°F (1770°C)	2957°F (1625°C)	Slightly too fluid to draw fibers.

*Could not read due to bubbles.

darkening, although probably not enough to create serious problems. Since La_2O_3 and Y_2O_3 are comparatively expensive, ZrO_2 was chosen as the first candidate. With this oxide as the only additive, the material did not seem to have good fiber forming properties. Addition of a third component was tried to bring about improvement in this respect. 10 w/o MgO did not seem to have the desired effect, but did reduce the viscosity drastically. 10 w/o Al_2O_3 improved fiber forming characteristics, but appeared to produce too great a reduction in the viscosity, while an addition of 5 w/o Al_2O_3 produced a glass which appeared to be very close to 5A-glass in viscosity and fiber forming ability. When this glass was tried in the bushing, however, it was found to be considerably less viscous than required. On the other hand, when the glasses containing 10 w/o La_2O_3 and 10 w/o Ta_2O_5 were melted in the bushing, both were found to have an acceptable viscosity, with the Ta_2O_5-containing glass slightly higher in viscosity than ideal. A considerable amount of fiber was drawn from each glass at approximately 3730°F (2055°C). The glass containing Y_2O_3 was not tried in the bushing. One intention in these experiments was of course to form core sheath fibers to observe any improvement brought about by the new glass compositions. But, because of the metallic deposit covering the nozzle and in particular the orifice (discussed earlier), the core material could not flow. Depletion of funds prevented remedial action and repetition of the experiments.

B. Core Compositions

It became apparent early in the program that Al_2O_3 had some undesirable physical properties for use in the core-sheath liquid phase process for producing oxide fibers. The major problem with Al_2O_3 was the approximately 24% reduction in volume which it undergoes when passing from the liquid to the solid state. It was felt that the large volume contraction upon solidification had to be reduced or eliminated to produce successful two phase oxide fibers. Modifications of the core composition were undertaken to solve this problem.

The use of Lucalox* alumina was discontinued in favor of reagent grade alumina in powder form to reduce cost, but more importantly to allow easy mixing with various additives. Additives which were tried while the short (0.5-inch) (1.27 cm) core orifice was still in use were 1 w/o Cr_2O_3, 2 w/o Fe_2O_3, 5 w/o Fe_2O_3 and 2.5 w/o MgO. The Cr_2O_3-addition had the unfortunate effect of breaking the fiber almost immediately upon injection into the forming cone, thus making fiber forming extremely difficult. In contrast, when either concentration of Fe_2O_3 was used, the core-sheath fiber was actually easier to draw than when using pure alumina. It was in this fiber that the first indication was seen that the core discontinuities may have been caused by a difference in thermal expansion between sheath and core, rather than by silica migration into the core. A core sheath fiber was formed with the MgO-addition, but with some difficulty. The

* General Electric Co.

tendency of this fiber to break during forming was intermediate between that of the one using pure alumina and the one using 1 w/o Cr_2O_3 in the core.

After the 0.9-inch (2.28 cm) core orifice nozzle had been tested successfully with pure alumina, several core compositions were tried. The Fe_2O_3-addition was increased to five and ten weight percent, and in each case core-sheath fibers were formed with ease. When the 1 w/o Cr_2O_3-addition was used again, fiber forming was virtually as difficult as when it was used with the short nozzle. On the other hand, an addition consisting of a combination of 5 w/o Cr_2O_3 and 5 w/o Fe_2O_3 permitted core-sheath fiber forming without difficulty. Apparently, the Fe_2O_3 compensated sufficiently for the detrimental effect the Cr_2O_3 has on the forming process. Core-sheath fibers were also drawn using the core compositions 20 m/o Sm_2O_3 in alumina and $3Y_2O_3 \cdot 5Al_2O_3$ (37.5 m/o Y_2O_3). Each of these oxides, Sm_2O_3 and Y_2O_3, has been shown [2] to reduce significantly the volume shrinkage exhibited by alumina during solidification. Besides mullite ($3Al_2O_3 \cdot 2SiO_2$) and spinel ($MgO \cdot Al_2O_3$), alumina compositions used were $Al_2O_3 \cdot TiO_2$, $BaO \cdot 6Al_2O_3$, and 40 w/o V_2O_5 in alumina. Core-sheath fibers were obtained with all of these, except possibly the last one where it is not certain that a core was obtained. Since the accepted value for the melting point of spinel is about 100°C higher than that for alumina, difficulties were anticipated but did not materialize; fibers with a spinel core were drawn in the range between 3713°F (2045°C) and 3766°F (2075°C), according to the optical pyrometer. The spinel core showed a certain amount of promise, and two small additions were used in attempts to further improve properties, 3 w/o TiO_2, and 3 w/o Cr_2O_3. In each case, core-sheath fibers were obtained.

V. FIBER EVALUATION

A. Fiber Defects

The discontinuities present in the core of most fibers were believed to be caused from three separate sources.

The first source of defects was the diffusion of SiO_2 into the Al_2O_3 core while both materials were in the liquid state. With the old short nozzle on the inner bushing, a large forming cone of SiO_2 was formed. The Al_2O_3 was injected into this mass of liquid SiO_2 while a glass fiber was being pulled. The Al_2O_3 would be carried along with the SiO_2 glass and pulled into a fiber. This process produced a relatively long contact time between the two materials at 3722°F (2050°C) where diffusion was inevitable. Also a certain amount of turbulence was present to cause further mixing. The compound derived from the mixing and diffusion was mullite which was found as inclusions in the core of the two phase fibers (Figure 1). It is believed that the mullite formed in the forming cone and agglomerated to completely fill the core cross section at discrete intervals. As stated earlier, this problem was solved primarily by extending the core nozzle to a point very close to the end of the glass forming cone. This equipment improvement decreased the time the two liquids were in contact, reduced the turbulance and minimized the amount of mullite formation.

The second and third problems were encountered after the mullite problem was eliminated. The further problems were associated with the approximately 24% volume shrinkage of the Al_2O_3 upon solidification and the thermal expansion mismatch between SiO_2 glass (0.5×10^{-6} per °C) and Al_2O_3 (9.0×10^{-6} per °C).

After the longer inner nozzle was successfully used to make core sheath fibers a new type defect was found, as shown in Figure 2. Both internal voids and cracks in the core were present. It became apparent that the effects of the volume shrinkage of Al_2O_3 were finally being observed. Since Al_2O_3 solidifies at a specific temperature, 3722°F (2050°C), while the glass solidifies over a rather broad temperature range, the Al_2O_3 core fiber was being subjected to a restraining tensile force by the glass sheath that is cumulative along the length of the core fiber. When the stress is sufficiently large the core fiber will fail and contract within the limits of further constraint by the glass sheath. Such a process would cause voids as shown in Figure 2. This process may have been in effect with the shorter nozzle but it was masked by the large amounts of mullite which were being formed. Further, since mullite solidifies at a lower temperature, 3288°F (1810°C), it could flow and prevent some voids which otherwise might have formed because of volume shrinkage, obscuring the primary cause of discontinuities in the core.

The last and equally important problem is thermal expansion mismatches between the core and sheath. Small cracks were also present in the core of many fibers which were the nucleation site for cracks initiation in the glass

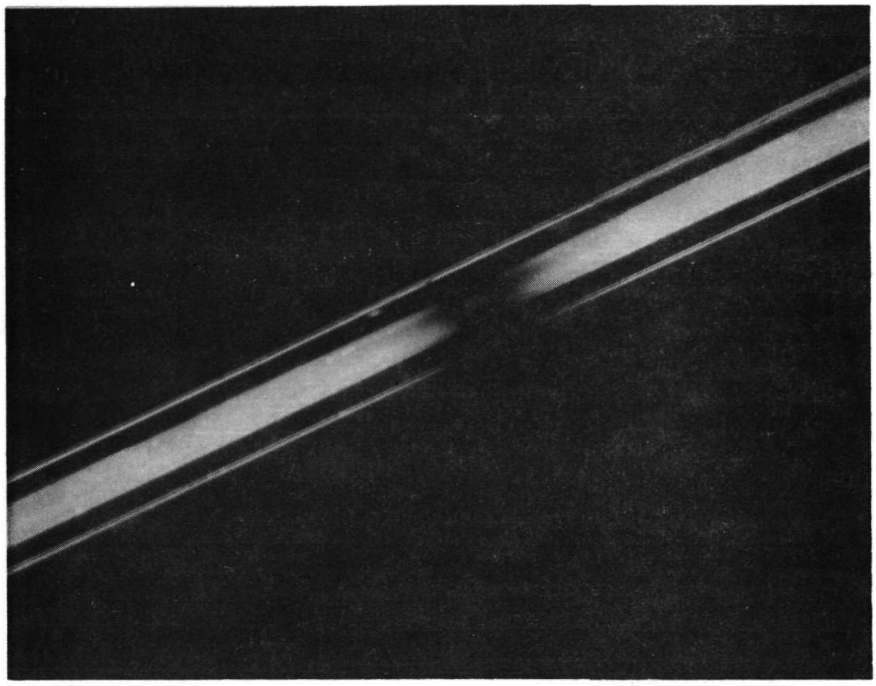

Figure 1. Core Discontinuity, Old Type (Magnification 88)

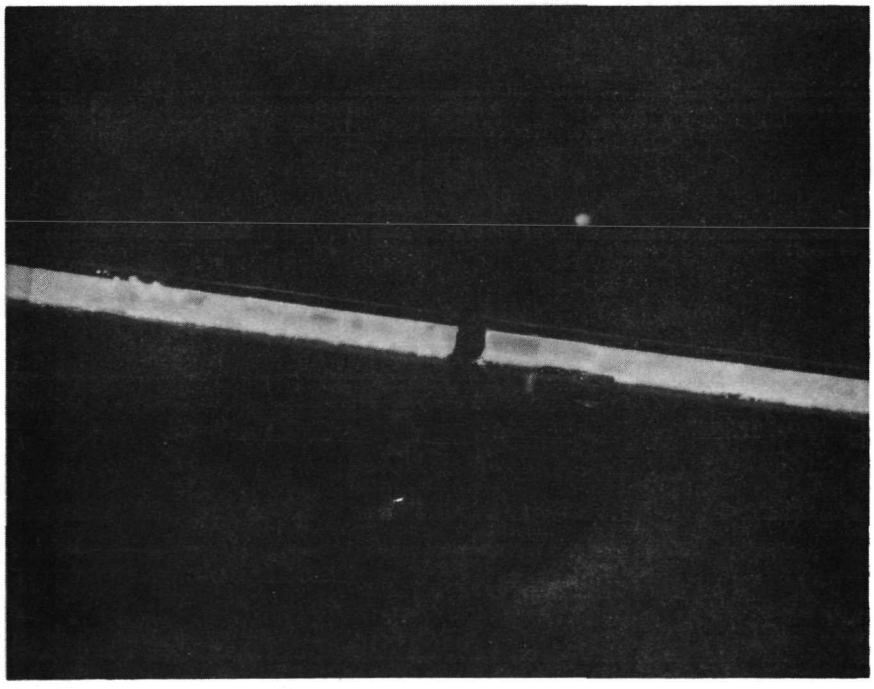

Figure 2. Core Discontinuity, New Type (Magnification 88)

sheath, Figure 3. This type of defect is a low temperature phenomenon which can be explained by the thermal expansion mismatch of the core and sheath. The stress that is built up by the mismatch increases as the fiber cools to room temperature. When the thermally induced stress reaches the point where core failures occur in tension, the glass is very stiff and cracking of the core is accompanied by crack propagation into the adjacent glass sheath. Of all the defects, this one is the most damaging since the propagation of the existing cracks is initiated at a relatively low stress. The early failures in the creep tests seem to indicate the presence of pre-existing microscopic cracks.

B. Fiber Defects as Effected by Composition

Even small modifications of the alumina core often had very marked effects. It has already been mentioned that only 1 w/o of Cr_2O_3 made core-sheath fiber forming virtually impossible. On the other hand, Fe_2O_3 in various concentrations not only facilitated forming, but also produced a fiber with core discontinuities which, although numerous, were of almost microscopic size; just barely detectable by direct visual examination. Under the microscope they also looked different from those commonly seen earlier (old type); instead of the usual tapering of opaque alumina into transparent sections, the boundaries of the new type were sharp and perpendicular to the fiber axis (Figures 1 and 2). They definitely looked like the result, not of silica diffusion, but of the contraction of the core being greater than that of the sheath. The 2.5 w/o MgO was added to the alumina in the hope of reducing the volume shrinkage, but apparently did not have the desired effect since the discontinuities persisted.

When the longer core orifice nozzle was used, this new type of discontinuity was more common than the old type even in cores containing pure alumina. When 5 w/o Fe_2O_3 was used with the longer nozzle, the frequency of discontinuities was greatly reduced from what it was when this material was used with the short nozzle. Thus, the long nozzle brought about an improvement both with respect to silica diffusion and fluid flow characteristics of the process. Increasing the Fe_2O_3 content to ten volume percent did not result in additional improvement, but combining 5 w/o Fe_2O_3 with with 5 w/o Cr_2O_3 did appear to further reduce the frequency of discontinuities. The two additives Y_2O_3 and Sm_2O_3 apparently had the desired effect of reducing the volume shrinkage of the alumina to a point where no discontinuities developed in the core. Not a single flaw could be detected in the core consisting of $3Y_2O_3 \cdot 5Al_2O_3$. This core was completely transparent, indicating a lack of devitrification. The core consisting of 20 m/o Sm_2O_3 in alumina was also basically transparent, but contained crystallites varying in size and abundance. In addition, it contained occasional bubbles, which were probably the result of either gas formation in the core or of a viscosity sufficiently high to prevent the escape of entrapped gas in the time available. In the case of the fiber with a mullite core, the core ranged from transparent to almost completely crystallized. Transparent cores were also obtained when spinel was used, but in some samples the core was white and opaque without any detectable flaws. Some very high core-to-sheath

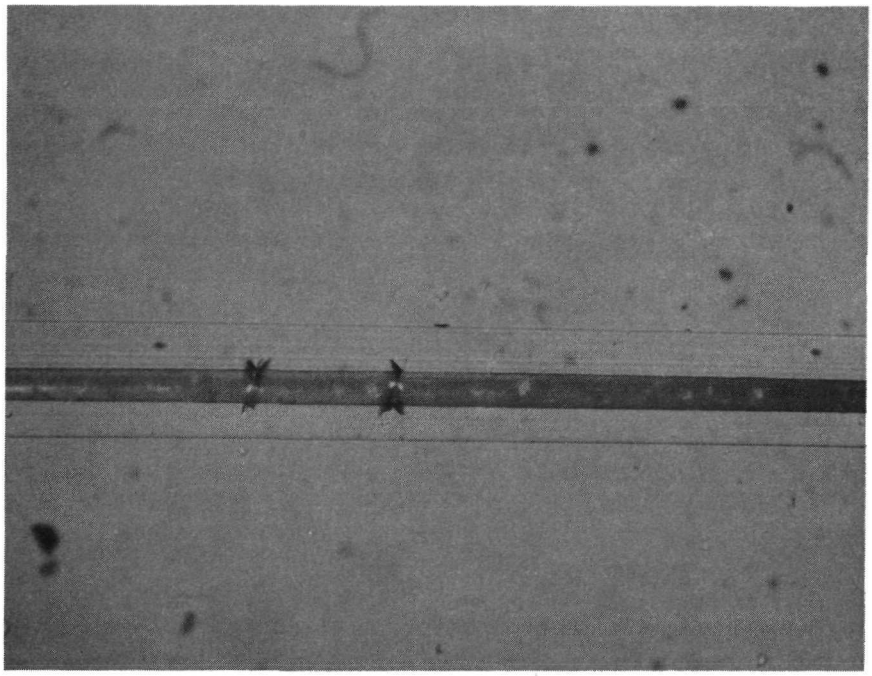

Figure 3. Small Cracks in Fiber Core Initiating Cracks in the Sheath

ratios were also obtained in the case of this fiber. The core consisting of $Al_2O_3.TiO_2$ was black or almost black, and appeared glassy and completely free of flaws. The core-to-sheath ratio was very large. When heated for a few seconds in the propane torch the core turned various shades of blue, from very dark to almost white. A fiber containing 3 w/o TiO_2 in spinel produced a core which was very similar in appearance to the $Al_2O_3.TiO_2$-core after the treatment in the torch. The core-to-sheath ratio was almost but not quite as large. Again, no flaws were detected and the TiO_2 thus appears to be very effective in eliminating core discontinuities. When 3 w/o Cr_2O_3 was added to spinel a pink core was obtained which contained discontinuities, and in the case of the $BaO{\cdot}6Al_2O_3$-core, discontinuities were plentiful. Testing at elevated temperature generally brough about devitrification in those cores which appeared glassy in the as-formed condition.

C. Creep and Tensile Strength

Creep and tensile strength data was first obtained for fibers with 3A-glass in the sheath and the following compositions in the core: 10 w/o Fe_2O_3 in alumina, 5 w/o Cr_2O_3 + 5 w/o Fe_2O_3 in alumina, $3Y_2O_3.5Al_2O_3$, 20 m/o Sm_2O_3 in alumina, $MgO{\cdot}Al_2O_3$ (spinel), and $3Al_2O_3$ $2SiO_2$ (mullite). Two samples of the yttria-containing fiber were tested for tensile strength at room temperature. One, with a diameter of 5.86 mils, gave a value of 49,000 psi (33.8N/cm^2) and the other, with a diameter of 6.64 mils, gave a value of 52,300 psi (36.1N/cm^2). These values are slightly higher than those obtained in the past for fibers with pure alumina cores under similar conditions. Actually, a considerably greater improvement was expected because yttria-containing fibers appear much stronger in handling. All the fibers were tested for creep and strength in tension at 2000°F (1093°C). As a check on the temperature of the testing furnace obtained with the otpical pyrometer, a thermocouple was inserted in the furnace, and the readings compared. The difference between the two was only 11°F (6°C). The tensile strength of each fiber was determined by increasing the load to the breaking point after the creep had been observed for a period of time at a lower stress level.

The data is presented in Table II. Core diameters were measured with the fiber immersed in anisole having an index of refraction of 1.52, which is close to that of the glass. The column headed "Stress" gives the stress at the point where the creep value shown was measured. In choosing this point, an attempt was made to keep the stress values within a fairly narrow range. In the case of two fibers (10 w/o Fe_2O_3 and mullite) two points were chosen to illustrate the effect of a change in the stress on the creep (not directly proportional). In calculating the stress, as in calculating the tensile strength, both the fiber diameter and the core diameter were used. Microscopic examination subsequent to the tests revealed gaps in the core in all fibers except the larger diameter spinel fiber and the fiber containing 20 m/o Sm_2O_3 in the core. At the locations of the gaps, attenuation in the glass was seen, while no decrease in the core diameter was detected. Thus, the observed creep apparently occurred in the glass rather than in the core, except in the case of the two fibers

TABLE II

FIBER PROPERTIES AT 2000°F (1093°C)

Core Material	Creep (10^{-4} min^{-1})	Stress				Diameter				Tensile Strength			
		Fiber		Core		Fiber		Core		Fiber		Core	
		10^3 psi	10^3 N/cm^2	10^3 psi	10^3 N/cm^2	mil	micron	mil	micron	10^3 psi	10^3 N/cm^2	10^3 psi	10^3 N/cm^2
5 w/o Cr_2O_3 + 5 w/o Fe_2O_3 in alumina	128	4.88	3.37	26.6	18.4	5.88	149	2.52	64.0	- (a)		- (a)	
10 w/o Fe_2O_3 in alumina	58.4	9.20	6.35	69.6	48.0	4.62	117	1.68	42.6	31.0	21.4	235	162
	10.5	4.60	3.17	34.8	24.0								
$3Y_2O_3 \cdot 5Al_2O_3$	72.2	4.53	3.12	12.2	8.41	4.66	118	2.84	72.1	13.6	9.38	43.0	29.7
20 m/o Sm_2O_3 in alumina	16.0	3.87	2.67	15.5	10.7	5.04	128	2.52	64.0	27.0	18.6	110	75.9
$MgO \cdot Al_2O_3$ (spinel)	0.584	5.05	3.48	12.8	8.83	7.35	187	4.62	117	12.7	8.76 (b)	32.2	22.2 (b)
	18.3	5.24	3.62	26.7	18.4	6.55	166	2.90	73.6	14.7	10.1 (c)	74.8	51.6 (c)
$3Al_2O_3 \cdot 2SiO_2$ (mullite)	43.8	5.78	3.99	38.0	26.2	4.41	112	1.72	43.7	32.5	22.4	246	170
	13.0	2.17	1.50	14.2	9.80								

(a) No tensile strength value was obtained for this fiber, since it was allowed to attenuate into failure. The highest stress applied during the creep test was 8,100 psi ($5.6 N/cm^2$) using the fiber diameter, and 45,000 psi ($31. N/cm^2$) using the core diameter.

(b) Jaw break.

(c) May have been a jaw break (portion of fiber missing after test).

noted above. In determining the tensile strength, the loading rate was quite high, and it is probable that the sheath was carrying its share of the load according to its relative cross section. The key to obtaining true values for both the creep and the tensile strength of the core appears to be a sufficiently slow loading rate to allow plastic deformation of the sheath to such an extent that it will carry only an insignificant portion of the load. Obtaining both creep and tensile strength data from the same sample saved time, but interfered with the microscopic examination of the samples subsequent to testing. It could not be ascertained whether cracks in sheath and core developed during the creep test or at the moment of failure, and furthermore, a portion of the fiber was often lost when it snapped, thus preventing a complete examination.

To test the next group of fibers, the testing procedure was modified for the reasons just discussed. In the new procedure, the load applied to the fiber was increased in steps, each step being equal to 20% of full scale deflection on the read-out equipment. The load was maintained at each level for approximately five minutes, long enough for virtually all the stress to be transferred to the core through plastic deformation in the glass sheath, and the creep was observed at each level. The data obtained at 20000°F (1093°C) is presented in Table III, and in choosing the data points here, an effort was made to keep the stress in the core within a narrow range.

Fibers were also tested at 1600°F (871°C) to determine their usefulness at this temperature. After testing fibers with cores consisting of 20 m/o Sm_2O_3 in alumina, and 3 w/o TiO_2 in spinel, both of which showed little or no creep at this temperature, it was decided to test a 3A-glass fiber, without core, for comparison. Surprisingly, this fiber showed no creep at 1600°F (871°C). All three fibers started to slip out of the Ceramabond 503* cement (fresh batch, just purchased) when a certain load level was reached; 190 gm, 160 gm, and 90 gm respectively, amounting to fiber stresses of 21×10^3 psi (14.5×10^3 N/cm^2), 12.8×10^3 psi (8.9×10^3 N/cm^2), and 12.0×10^3 psi (8.3×10^3 N/cm^2). Two more 3A-glass fibers without cores were tested at 1600°F (871°C) but here, fibers long enough to be attached directly to the tester jaws, outside the furnace, were used. The target for the optical pyrometer was a small bead of Ceramabond 503 placed on the fiber in the middle of the furnace. No creep was observed, and no slip occurred, but the fibers broke at low stress levels, 23.6×10^3 psi (16.3×10^3 N/cm^2) and 30.0×10^3 psi (20.7×10^3 N/cm^2). It should be noted that in each case the break occurred, not while the load was being increased, but after it had been maintained at the failure level for two and three minutes. The tensile strength of 3A-glass fibers with little or no core was also determined at room temperature. Ten samples were used, and the values were, in order of decreasing strength, 120×10^3 psi (82.7×10^3 N/cm^2), 120×10^3 psi (82.7×10^3 N/cm^2), 103×10^3 psi (71.0×10^3 N/cm^2), 96.0×10^3 psi (66.2×10^3 N/cm^2), 84.8×10^3 psi (58.5×10^3 N/cm^2), 76.3×10^3 psi (54.6×10^3 N/cm^2), 73.6×10^3 psi (50.7×10^3 N/cm^2), 73.2×10^3 psi (50.4×10^3 N/cm^2), 65.4×10^3 psi

* Aremco Products, Inc.

TABLE III

FIBER PROPERTIES AT 2000°F (1093°C)

Core Material	Creep (10^{-4} min^{-1})	Stress*				Diameter			
		Fiber		Core		Fiber		Core	
		10^3 psi	10^3 N/cm^2	10^3 psi	10^3 N/cm^2	mil	micron	mil	micron
$Al_2O_3 \cdot TiO_3$	54.1	2.49	3.61	9.83	6.78	4.75	121	2.39	60.7
3 w/o TiO_2 in spinel	4.23	4.25	2.93	8.52	5.88	6.30	160	4.45	113
3 w/o Cr_2O_3 in spinel	27.6	-	-	8.82	6.09	-	-	3.57	90.6
$BaO \cdot 6Al_2O_3$	10.2	4.97	3.43	9.50	6.56	2.06	52.3	1.49	37.8
40 w/o V_2O_5 in alumina	207	4.11	2.83	-	-	1.85	47.0	-	-

* Stress at point where creep was measured.

(45.1×10^3 N/cm^2), and 41.7×10^3 psi (38.8×10^3 N/cm^2). It must be noted that these fibers were taken from bundles, and had therefore been subjected to severe abrasion.

D. X-Ray Diffraction Analysis

X-ray diffraction spectra were obtained for two fibers containing a spinel core, one in the as-formed condition, and one after creep and strength testing at 2000°F (1093°C). In the first case a spectrum was obtained which closely resembled one for a magnesium aluminum oxide described on the card as: "Metastable intermediate phase related to the spinel structure. Chemical composition unknown. Observed only for synthetic spinels of molar ratios $MgO:Al_2O_3$ larger than 1:2.5." In a later experiment a very similar spectrum was obtained for the starting material, supposedly a natural spinel. The spectrum given for spinel ($MgO \cdot Al_2O_3$) is considerably different. Visual examination of the second sample revealed that the sheath had turned opaque during the heat treatment. A definite spectrum for α-cristobalite (SiO_2) was obtained, and in addition, a trace of mullite was indicated. These spectra were in all probability produced by the crystallized sheath, which apparently did not allow the X-rays to penetrate to the core.

A section of a fiber with a Vycor sheath, and a core composition consisting of Al_2O_3 and SiO_2 in a moler ratio of 3:2, mixed with the intention of forming mullite, was analyzed. Most of the glass sheath had broken off, leaving the well devitrified core bare. The spectrum obtained was not a mullite spectrum as expected, but that of a fairly recently reported [3] form of alumina (ϵ-alumina) which is only stable above 3505°F (1930°C).

VI. DISCUSSION OF RESULTS

Of the fibers listed in Table II, the most interesting were of course the two which did not show any gaps in the core following testing. Of these, the fiber containing 20 m/o Sm_2O_3 showed too much creep at 2000°F (1093°C) to be useful at this temperature. The value for the creep of the large diameter spinel fiber given in Table II is a maximum value. The small creep was taxing the sensitivity of the readout equipment, and the total change in the trace on the recorder chart, reflecting the creep, was comparable to the random fluctionations. Thus, the actual creep may have been considerably smaller. One source gives a value for the creep of spinel of $0.439 \times 10^{-5} min^{-1}$ at a stress of 1800 psi (12.4 N/cm^2) and a temperature of 2370°F (1300°C). This value is about one order of magnitude smaller than the value given in Table II, but at least part of this is accounted for by the fact that the stress level is considerably lower. The temperature is higher, but not by as much as it appears; our value of 2000°F (1093°C) is an uncorrected optical pyrometer reading and is low due to the fact that perfect black-body conditions did not prevail.

The high creep displayed by the first and last fibers in Table III appeared to be the result of attenuation rather than breaks in the core. Examination under the microscope before and after testing showed great attenuation in the Al_2O_3 TiO_2-core. Thus, this material is not suitable for applications at 2000°F (1093°C). As mentioned earlier, it is not certain whether a core-sheath fiber was produced when using 40 w/o V_2O_5 in alumina, since no core could be seen during or following forming. After testing at 2000°F (1093°C), what appeared to be a core could be seen but it looked glassy and had been drawn into a point, thus indicating that the material is of no use at 2000°F (1093°C). In the case of the fiber with a core consisting of $BaO{\cdot}6Al_2O_3$, there was some difficulty in determining whether the creep was caused by attenuation or breaks in the core, but in either case, the material appears unsuitable for applications at 2000°F (1093°C). In the case of both fibers where small additions to the spinel core were used, breaks were seen in the core subsequent to testing. The performance of the TiO_2- addition being superior to that of the Cr_2O_3-addition was somewhat surprising. Both additions failed to improve the properties of the pure spinel, and may in fact have been detrimental.

No improvement in the low strength displayed by the 3A-glass fiber at 1600°F (871°C) could be expected simply by the addition of a core. A fracture traveling from the fiber surface toward the center at catastrophic speed and carrying with it an extremely high stress concentration would certainly not be stopped by a brittle, ceramic core. Thus, at this temperature, tensile strength tests measure the strength of the glass rather than that of the core. At 2000°F (1093°C) the situation is different in that here the viscosity of the glass is low enough to allow flaws to be healed through plastic flow. Points of high stress concentration would not develop unless the rate of load application is sufficiently rapid to make the glass still behave as a brittle material.

VII. CONCLUSIONS AND RECOMMENDATIONS

Production of high strength core-sheath fibers is possible only after solution of the problem of the core discontinuities resulting from the large volume shrinkage of pure alumina during solidification. Shrinkage discontinuities may be eliminated by using core compositions with reduced solidification shrinkage, which may or may not contain alumina. Of the compositions tried in this program, the most promising one appears to be spinel ($MgO \cdot Al_2O_3$). Small additions to this material should be used in attempts to further improve its properties.

One might conclude from the creep data in Table II and Table III that creep is a serious problem at 2000°F (1093°C), but this is not actually the case. Attenuation of the core was observed only in the case of the core compositions 20/mo Sm_2O_3, $Al_2O_3 \cdot TiO_2$, and probably 40 w/o V_2O_5, and it may have occurred with $BaO \cdot 6Al_2O_3$. In all other cases, with the exception of the large diameter spinel core, the creep was caused by breaks in the core which allowed the glass to attenuate. Thus, the real problem is not creep, but low core strength which may be due to microscopic cracks in the core. It should be noted in Table II that even the fiber with the large diameter spinel core displayed low strength. In several instances, the recorder traces showed that breaks must have occurred just at the beginning of the creep test, or been present already. In the latter case, the breaks would have had to be merely discontinuities in the structure, too small to be seen even under the microscope. Either condition could easily be brought about by the large difference in thermal expansion coefficient between sheath and core which, during the rapid quenching associated with forming, introduces severe tensile stresses in the core. Thus, the low core strength may be the result of core discontinuities of a different nature and origin than those which were eliminated by replacing pure alumina with other core compositions, and it is quite probable that the core strength could be greatly improved by a closer match between the thermal expansion of sheath and core. Since it is highly improbable that the expansion coefficient of the core could be reduced to the exceptionally low value of the coefficient of the high-silica sheath, the only practical alternative is to attempt to increase the latter sufficiently. The expansion coefficients of the fibers already drawn from the three glass compositions mixed with high thermal expansion in mind should be measured. If necessary, more fibers should be formed from other selected compositions and tested. A close match in thermal expansion would not only be expected to produce a stronger fiber, but also to reduce the frequency of breaks occurring during forming and thus make fiber production more continuous and economical.

Several possible improvements in the forming process itself have also become obvious during the performance of this work. Fiber forming with the longer core orifice nozzle is now marginal when an iridium sheath bushing is used. If a glass composition requires iridium containment in order not to suffer discoloration, however, several measures can be taken to make the operation less marginal. Instead of using a ceramic support as in the

past, the bushing can be placed in a tungsten cup supported by three legs consisting of 1/4-inch (0.635 cm) tungsten rod. The smaller bulk, larger spacings, and higher thermal conductivity of this support would allow considerably more heat to reach the nozzle. Even more effective would be the use of a heating element with a larger diameter than in the past. The heat from any hot spot developing on the element would then be distributed over a large area of the bushing rather than concentrated in a small region causing localized melting. A further improvement in the forming process would consist of changing the sight hole into a vertical slit which would allow examination during forming of not only the forming cone but also the upper portion of the fiber. This is a critical region, because in many instances where core material has been seen to be present in the forming cone, the fiber has subsequently been found to be devoid of core.

REFERENCES

1. Volf, M.B., Technical Glasses, Sir Isaac Pitman and Sons, LTD, London, SNTL, Publication os Technical Literature, Prague, 1961, pp. 23, 24.

2. J. Lambert Bates and J. J. Rasmussen, Effects of Additives on Volume Change on Melting, Surface Tension, and Viscosity of Liquid Aluminum Oxide, Final Report, NASA Contract NAS 3-14308, Battelle Memorial Institute, 1971.

3. Cevales, G., Das Zustandsdiagramm Al_2O_3-ZrO_2 und die Bestimmung einer neuen Hochtemperaturphase (α-Al_2O_3), Ber. Deut, Keram. Ges., 45, 216 (1968).

4. J. F. Lynch, et al., Engineering Properties of Ceramics, AFML-TR-66-52, Battelle Memorial Institute, 1966.

DISTRIBUTION LIST

(The number in parentheses is the number of copies sent to each addressee.)

NASA Headquarters
600 Independence Avenue
Washington, D. C. 20546
Attn: N. F. Rekos (RAP) (1)
G. C. Deutsch (RR-1) (1)
R. H. Raring (RRM) (1)
J. J. Gangler (RRM) (1)

NASA-Lewis Research Center
21000 Brookpark Road
Cleveland, Ohio 44135
Attn: Technology Utilization Office, MS 3-19 (1)
John Weeton, MS 49-3 (1)
G. M. Ault, MS 3-13 (1)
R. W. Hall, MS 105-1 (1)
Library, MS 60-3 (2)
Report Control Office, MS 5-5 (1)
H. B. Probst, MS 49-3 (1)
R. A. Signorelli, MS 106-1 (1)
L. J. Westfall, MS 106-1 (44)
R. H. Kemp, MS 49-3 (1)
E. J. Kelman, MS 500-313 (1)

FAA Headquarters
800 Independence Avenue, SW
Washington, D. C. 20553
Attn: Brig. Gen. J. C. Maxwell (1)

NASA Scientific and Technical Information Facility (6)
P. O. Box 33
College Park, Maryland 20740

U. S. Atomic Energy Commission
Washington, D. C. 20545
Attn: Technical Reports Library (1)
Jules Simmons (1)

Air Force Office of Scientific Research (1)
Propulsion Research Division
USAF Washington, D. C. 20525

Defense Documentation Center (DDC) (1)
Cameron Station
5010 Duke Street
Alexandria, Virginia 22314

Headquarters
Wright-Patterson AFB, Ohio 45433
Attn: MAAM - Technical Library (1)
AFSC-FTDS (1)
AFML-A. M. Lovelace (1)
SESOS (1)

Department of the Navy
ONR
Code 429
Washington, D. C. 20525
Attn: Dr. R. Roberts (1)

U. S. Army Aviation Materials Laboratory
Fort Eustis, Virginia 23604
Attn: John White, Chief, SMOFE-APG (1)

Chief, Bureau of Naval Weapons
Department of the Navy
Washington, D. C. 20525
Attn: T. F. Kearns (1)

NASA-Langley Research Center
Langley Field, Virginia 23365
Attn: Library (1)
Richard Pride (1)

NASA-Marshall Space Flight Center
Huntsville, Alabama 35812
Attn: Library (1)

Jet Propulsion Laboratory
4800 Oak Grove Drive
Pasadena, California 91102
Attn: Library (1)

Army Materials Research Agency
Watertown Arsenal
Watertown, Massachusetts 02172
Attn: S. V. Arnold, Director (1)

NASA-Ames Research Center
Moffett Field, California 94035
Attn: Library (1)

NASA-Goddard Space Flight Center
Greenbelt, Maryland 20771
Attn: Library (1)

NASA-Manned Space Flight Center
Houston, Texas 77058
Attn: Library (1)
NASA-
NASA-Flight Research Center
P. O. Box 273
Edwards, California 93523
Attn: Library (1)

Defense Metals Information Center
(DMIC) (1)
Battelle Memorial Institute
505 King Avenue
Columbus, Ohio 43201

General Electric Company
Advanced Technology Laboratory
Schenectady, New York 12305
Attn: Library (1)

General Electric Company
Materials Development Laboratory
Operation
Advanced Engine and Technology
Department
Cincinnati, Ohio 45215
Attn: L. P. Jahnke (1)

General Motors Corporation
Allison Division
Indianapolis, Indiana 46206
Attn: D. K. Hanink, Materials
Laboratory (1)

Stanford University
Palo Alto, California 94305
Attn: Prof. Oleg Sherby, Dept.
of Mat'l. Science (1)

United Aircraft Corporation
400 Main Street
East Hartford, Connecticut 06108
Attn: E. F. Bradley, Chief
Mat'l.s Eng. (1)

United Aircraft Corporation
Hamilton Std. Division
Windsor Locks, Conn. 06096
Attn: H. P. Berie (1)

Lockheed Mississippi Space Co.
Palo Alto Research Lab.
Palo Alto, California
Attn: Alde Videz (1)

Lockheed-Georgia
Dept. 72-14
Marietta, Georgia 30060
Attn: Dr. W. Cremens, Zone 402 (1)

Clevite Corporation
7000 St. Clair Avenue, N.E.
Cleveland, Ohio 44110
Attn: G. F. Davies (1)

Maggs Research Center
Watervliet Arsenal
Watervliet, N. Y. 12189
Attn: Dr. I. Ahmad

NASA-Langley Research Center
Langley Station
Hampton, Virginia 23365
Attn: John Buckley (1)

General Electric AETD
Evandale, Ohio 45215
Attn: Dr. W. H. Chang (1)

E. B. Summers (1)
Harvey Engineering Labs.
Harvey Aluminum Co.
19200 S. Western Avenue
Torrance, California 90509

J. Bartos (1)
General Electric AETD
Evandale, Ohio 45215

W. A. Compton
Solar Division Int. Harvester
2200 Pacific Highway
San Diego, California

Dr. M. A. Decrescente (1)
Chief, High Temp. Mat.
United Aircraft Research Lab
East Hartford, Conn. 06108

Dr. F. S. Galasso (1)
Chief, Mat. Syn. Sec.
United Aircraft Research Lab
East Hartford, Conn. 06108

G. C. Grimes (1)
Southwest Research Ins.
8500 Culebra Road
San Antonio, Texas 78206

Dr. M. Ferman (1)
Allison Division, GMC
Department 5827
P. O. Box 894
Indianapolis, Indiana 46206

K. R. Hanby (1)
Battelle Memorial Institute
505 King Avenue
Columbus, Ohio 43201

H. Herring (1)
NASA-Langley Research Center
Structure Research Division
Langley Station
Hampton, Virginia 23355

Dr. K. G. Kreider (1)
United Aircraft Research Lab
East Hartford, Conn. 06108

Major Jon Kershaw (1)
MAMS
Wright-Patterson Air Force Base
Ohio 45304

Dr. R. H. Krock (1)
P. R. Mallory Co.
Northwest Industrial Park
Burlington, Mass. 01803

D. P. Laverty (1)
Section Mgr., Mat. Tech.
Equip. Labs., Div. of TRW
23555 Euclid Avenue
Cleveland, Ohio 44117

Dr. E. M. Lenoe (1)
Avco Corporation
Lowell Industrial Park
Lowell, Mass. 01850

Dr. S. R. Lyon (1)
AFML (MAMS)
Wright-Patterson Air Force Base

Dr. A. G. Metcalfe (1)
Solar Division
Int. Harvester Co.
2200 Pacific Highway
San Diego, California

A. Lawley (1)
Drexel Inst. of Tech.
Dept. of Metals Engineering
32 and Chustnut Streets
Philadelphia, Pa. 19104

A. P. Levitt
Army Mat./Mech. Research
Watertown, Mass. 02172

L. McCreight (1)
General Electric Co.
Valley Forge Space Tech.
P. O. Box 8555
Philadelphia, Pa. 19101

Librarian, Lycoming Div. (1)
AVCO Corp.
550 South Main Street
Stratford, Conn. 06497

G. D. Menke (1)
Honeywell, Inc.
Minneapolis, Minn. 55400

R. G. Moss (1)
Jet Propulsion Lab.
4800 Oak Grove Road
Pasadena, California 91103

Technical Librarian (1)
North American-Rockwell
4300 E. 5th Avenue
Columbus, Ohio 43216

Dr. M. J. Salkind (1)
United Aircraft Corp.
Sikorsky Aircraft Division
Stratford, Conn. 06497

Capt. W. A. Schulz (1)
AFMU
Wright-Patterson AFB
Ohio 45304

J. C. Weithers (1)
Gen. Tech. Corp.
1821 Michael Faraday Dr.
Reston, Virginia 22070

R. T. Pepper (1)
Aerospace Corp.
Bldg. H1, MS 2281
P. O. Box 95085
Los Angeles, California 90045

H. Shimizu (1)
Marquardt Corp.
16555 Saticoy St.
Van Nuys, California 91409

A. Toy (1)
Material Sciences Dept.
TRW Systems Group
One Space Park
Redondo Beach, California 90278

W. Wolkowitz (1)
Grumman Aircraft Eng.
Bethpage, Long Island
New York 11714

R. K. Robinson (1)
Ceramics/Composites Div.
Battelle-Northwest
3000 Stevens Drive
Richaldn, Washington 99352

Prof. E. Scala (1)
Bard Hall
Cornell University
Ithaca, New York 14850

Dr. D. M. Schuster (1)
Sandia Corporation
Metallurgy Div. 5431
P. O. Box 5800
Albuquerque, N. M. 87115

B. A. Wilcox (1)
Metal Science Group
Battelle Memorial Inst.
505 King Street
Columbus, Ohio 43201

A. J. Yeast (1)
Space Division
North American-Rockwell
12214 Lakewood Blvd.
Downey, California 90241

William C. Jurevic
Advanced Composites Information Center
Lockheed-Georgia Company
D/72-14 Zone 402
Marietta, Georgia 30060

Jack H. Ross (1)
AFML (Fiberous Materials Branch)
Wright-Patterson Air Force Base
Ohio 45433

Owens-Corning Fiberglass Corp. (1)
Technical Center
Granville, Ohio 43023
Attn: Miss B. J. Nethers (Librarian)

Rutgers University (1)
School of Ceramics
University Heights Campus
New Brunswick, N. J. 08903
Attn: Prof. W. H. Bover

United Aircraft Corporation (1)
Pratt & Whitney Div.
West Palm Beach, Florida 33402
Attn: Library

R. E. Tressler
(MAMS) Metals and Ceramics Div.
Wright-Patterson Air Force Base
Ohio 45304

Col. Lee R. Standfor - retired
Research and Technology
Armco Steel Corp.
Curtis Street
Middle Town, Ohio

Tyco Laboratories, Inc.
Waltham, Massachusetts 02154
Attn: H. E. LaBelle, Jr. (1)
G. H. Hurley (1)

A. Lopez
AFML/LTN
Wright-Patterson Air Force Base
Ohio 45433